Theoretical Investigation of CO₂ Adsorption on Graphene

Kun-Joon Lee and Seung-Joon Kim[*]

Department of Chemistry, HanNam University, Daejeon 300-791, Korea. [*]E-mail: sjkim@hnu.kr
Received October 24, 2012, Accepted July 21, 2013

The adsorption of carbon dioxide on graphene sheets was theoretically investigated using density functional theory (DFT) and MP2 calculations. Geometric parameters and adsorption energies were computed at various levels of theory. The CO_2 chemisorption energies on graphene-**C_{40}** assuming high pressure are predicted to be 71.2-72.1 kcal/mol for the lactone systems depending on various C-O orientations at the UCAM-B3LYP level of theory. Physisorption energies of CO_2 on graphene were predicted to be 2.1 and 3.3 kcal/mol, respectively, at the single-point UMP2/6-31G** level of theory for perpendicular and parallel orientations.

Key Words : DFT, Graphene, CO_2 adsorption, CAM-B3LYP

Introduction

It is well known that the vast usage of carbon-based fossil fuels has caused an increase in the concentration of atmospheric carbon dioxide (CO_2). This seems to be the major reason for the average global surface temperature rise of 0.6 °C over the past century.[1] Efforts to reduce the greenhouse gas CO_2 has been one of the most challenging issues in environmental protection. To solve this problem, there have been many investigations to control CO_2 emissions by capturing and separating technologies such as absorption, adsorption, membranes and so forth.[2] Among them, adsorption technologies using metal oxide, zeolite, or activated carbons *etc.* have been developed.[3] In recent years, the adsorption of various atmospheric gases including CO_2 on carbon nanotubes (CNT) or graphene as a candidate of adsorber beds has been experimentally and theoretically investigated.[4-19]

Some past researches for the single-walled carbon nanotube (SWNT) and metal-doped CNT have focused on the adsorption of H_2 as a candidate of hydrogen storage materials.[4-7] Also, studies on the electronic properties of SWNTs exposed to various gases such as O_2, NO_2, and NH_3 have been followed to demonstrate the possibility of becoming a nanotube molecular sensor.[8,9] The investigation on the adsorption of gases on SWNT expanded to more various gases (NO_2, O_2, NH_3, N_2, CO_2, CH_4, H_2O, H_2, Ar) using the first principle methods in Zhao *et al*.'s 2002 work.[10] The adsorption (physisorption) energy of CO_2 gas on purified SWNTs has been experimentally measured and theoretically predicted by Cinke *et al.* in 2003.[11] Experimental and theoretical investigation for the mechanism of CO_2 chemisorption on carbonaceous surfaces has been presented to understand the detailed gasification mechanism and surface characterization on graphene planes by Montoya *et al.* in 2003.[12] In the low-coverage region, their experimental adsorption energy varies from 75 to 24 kcal/mol, depending on binding sites and carbon-oxygen interactions such as lactone, heterocyclic, and furan-type complexes. In the same year, Matranga *et al.*

reported the result of the IR spectroscopic study of trapped CO_2 in SWNT bundles.[13]

Since single-layer graphene sheets have been successfully produced in experiments by Geim and coworkers in 2004,[14] intensive investigations on the fundamental properties of graphene-based structures have been initiated. Johnson and coworkers reported the experimental and theoretical adsorption energies and vibrational frequencies of CO_2 adsorbed at different sites on SWNT bundles and on graphene surface.[15] In 2005 Radovic reported the theoretical results on the mechanism of CO_2 chemisorption on zigzag carbon active sites in a graphene layer.[16] In the following year, the adsorption energies of various atmospheric gases including CO_2 on a single atom defected graphite surface was predicted using the ONIOM DFT method by Allouche and Ferro.[17] Also, Irle and coworkers have presented the prediction of reaction pathways and rate constants for the dissociative adsorption of CO_x and NO_x (x = 1-2) on the $C_{96}H_{24}$ graphene model using the ONIOM DFTB-D method.[18] In 2008, the adsorption of gas molecules (CO, NO, NO_2, O_2, N_2, CO_2, and NH_3) on graphene nanoribbons (GNRs) was studied by Duan and coworkers.[19] More recently, Cabrera-Sanfelix reported the binding energy of ~136 meV for physisorption and approximately 1.4 eV for chemisorption by the lactone group formation of CO_2 on a defective graphene sheet.[20] Last year, the physisorption and chemisorption energy were predicted to be ~210 meV and ~1.72 eV, respectively, for CO_2 adsorption on the defective graphene site with one carbon atom missing (monovacancy) by Liu and Wilcox.[21] Also, Mishra and Ramaprabhu have demonstrated the CO_2 adsorption capacity of graphene, prepared *via* hydrogen induced exfoliation of graphitic oxide at moderate temperatures. They confirmed the physical adsorption of CO_2 in graphene by FTIR study.[22]

This work reports DFT and MP2 calculations of the chemisorption and physisorption of CO_2 on graphene sheets. Three models of graphene sheet are considered, C_{32} (3-4-3) and C_{40} (4-5-4); geometric parameters and adsorption energies are calculated at various levels of theory. Harmonic

vibrational frequencies are also predicted to confirm that the optimized geometries are true minima.

Theoretical Approach

The possible structures of the graphene models are fully optimized at the B3LYP[23] level using the 6-31G** basis set. A long-range corrected (LC) DFT method, CAM-B3LYP,[24] in Gaussian-09[25] is also used for better description of the weakly binding physisorption of CO_2 on graphene sheets and compared with results from MP2 calculations. Harmonic vibrational frequencies are evaluated using analytic second energy derivatives at the B3LYP, CAM-B3LYP, and MP2 levels with the 6-31G** basis set. MP2 binding energies are obtained using single-point energy calculations at the B3LYP-optimized geometries. All possible high spin electronic states have been examined to find the ground state using the unrestricted wavefunction such as UB3LYP, UCAM-B3LYP and UMP2. All optimized geometries are confirmed to be true minima by all real frequencies.

The two models of graphene sheet are constructed using either three or four lines of benzene rings. For example, the C_{32} (3-4-3) case has three benzene rings in the first row, four rings in the second line, and three in the last, consisting of a total of 32 carbon atoms. Binding energies were calculated for chemisorption by the formation of lactone groups by CO_2 on the graphene sheets. Two orientations of physisorption – perpendicular and parallel – are investigated depending on the direction of CO_2's approach to the graphene. Adsorption energies are calculated using E(graphene-CO_2) {E(CO_2) + E(graphene)}. Zero-point vibrational energies (ZPVEs) are considered and compared with experimental adsorption energies. All computations were carried out using the Gaussian09 program package.

Results and Discussion

Structures. The geometric parameters for the chemisorption of CO_2 on the graphene-C_{32} at various levels of theory are listed in Table 1 and the optimized structure at the UB3LYP/6-31G** level of theory is presented in Figure 1(a). The formation of lactone groups has been reported to be the most exothermic process of CO_2 chemisorption on a zig-zag graphene model.[12] In the adsorbed CO_2, the bond length (R_3) between the central C atom and the O atom directly bonded to the graphene-C_{32} is calculated to be 1.44

Å, much longer than the 1.14 Å of pure CO_2. The other C-O bond length (R_4) is predicted to be 1.20 Å, still a little longer than that of pure CO_2. The ∠OCO bond angle is calculated to be 120.9°. The bonds between the CO_2 and the graphene surface are calculated to be 1.48 Å for C-C and 1.37 Å for C-O. The C-C bonds in the benzene ring at the outer edge of the graphene-C_{32} varied in length from 1.24 to 1.42 Å. The C-C bond lengths in the inner ring show less variation, ranging from 1.42 to 1.44 Å and showing a perfect plane. The structure generated by UCAM-B3LYP calculation is not too different from that generated by B3LYP, which means it is not very helpful in describing chemisorption, despite it being useful to characterize weakly bound long-range interactions such as physisorption.

The geometric parameters for the chemisorption of CO_2 on graphene-C_{40} at various levels of theory are also listed in Table 1. The optimized structures at the UB3LYP/6-31G** level of theory are shown in Figure 1(b, c). There are two similar but distinct active binding sites at which lactone groups can form during CO_2 chemisorption on graphene-C_{40} surface: site A at the graphene's outer edge and the inner site B. The bond between the carbon of the adsorbed CO_2 and its O atom directly bonded at site A to a graphene carbon (1.45 Å) is predicted to be slightly longer than those calculated

(a) $C_{32}CO_2$ (site A)

(b) $C_{40}CO_2$ (site A)   (c) $C_{40}CO_2$ (site B)
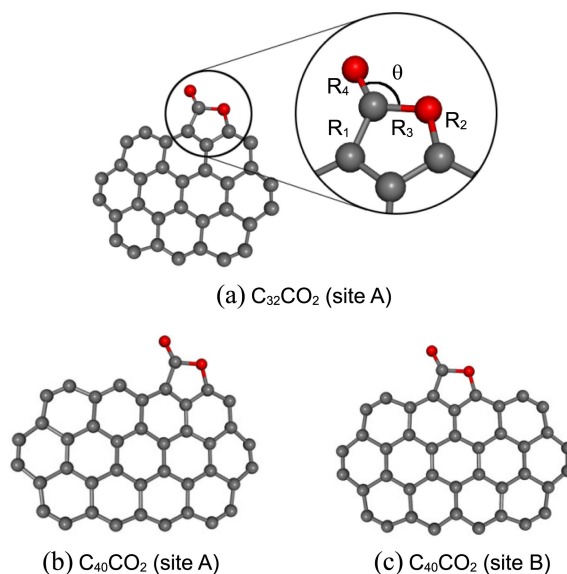
Figure 1. The optimized structures of CO_2 chemisorption on the graphene at the UB3LYP/6-31G** level of theory.

Table 1. Geometric parameters for CO_2 chemisorption on graphene sheets at various levels of theory

	$C_{32}CO_2$(A)		$C_{40}CO_2$(A)		$C_{40}CO_2$(B)	
	UB3LYP	CAM-UB3LYP	UB3LYP	CAM-UB3LYP	UB3LYP	CAM-UB3LYP
R_1(C-C)	1.48	1.48	1.47	1.48	1.48	1.48
R_2(C-O)	1.37	1.37	1.37	1.36	1.37	1.36
R_3(C-O)	1.44	1.42	1.45	1.43	1.44	1.42
R_4(C-O)	1.20	1.19	1.20	1.19	1.20	1.19
θ(O-C-O)	120.9	121.3	120.6	120.9	120.9	121.3
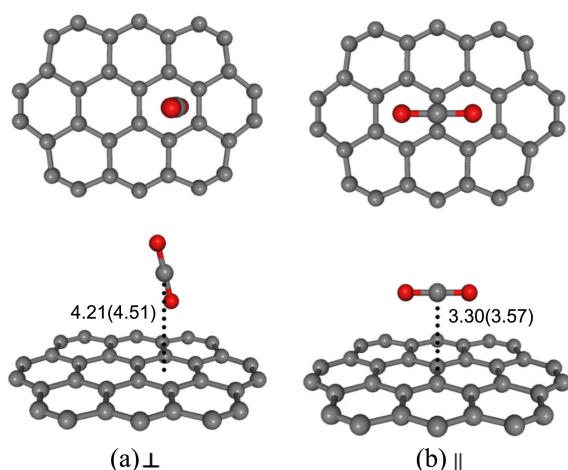
Figure 2. The optimized structures of CO_2 physisorption on the graphene-C_{32} at the UCAM-B3LYP/6-31G** (UB3LYP/6-31G**) level of theory (⊥: Located perpendicular on the graphene sheet, ‖ : Located parallel on the graphene sheet.

using a C_{32} model. All the other C-O bond lengths at sites A and B are calculated to be close to those calculated using the C_{32} model. The C-C bonds in the benzene rings at the outer edge of the C_{40} surface vary in length from 1.23 to 1.41 Å. The C-C bonds away from the edge are almost similar (1.41-1.44 Å) and show an undistorted plane.

The optimized structures of CO_2 physisorption on the graphene-C_{32} at the UCAM-B3LYP/6-31G** and UB3LYP/6-31G** levels of theory are shown in Figure 2. There are two optimized configurations, parallel (‖) and perpendicular (⊥), depending on the direction of the CO_2's approach to the surface. An oxygen atom of the CO_2 approaches the center of the benzene ring in both configurations. In the parallel

configuration, the carbon atom of CO_2 is oriented in the direction of the C-C bond of the benzene ring. The shortest distances between the carbon atom of the CO_2 and the graphene's surface are predicted at the UB3LYP/6-31G** level of theory to be 4.51 Å for the perpendicular configuration and 3.57 Å for the parallel configuration. They are reduced to 4.21 Å and 3.30 Å, respectively, at the UCAM-B3LYP/6-31G** level of theory. As expected, the UCAM-B3LYP result (3.3 Å) for the ‖ configuration is in better agreement with the experimentally observed 3.2 Å. The distances between CO_2 and the graphene are calculated to be 4.28 Å for the ⊥ configuration and 3.30 Å for the ‖ configuration on both the C_{40} surface at the UCAM-B3LYP/6-31G** level of theory (refer to Figure S1 in supplemental material). The differences between the calculated distances between the adsorbed CO_2 and each of the graphene surfaces are not sufficiently significant to make the simplest C_{32} surface inadequate for modeling the physisorption of CO_2 on graphene.

Adsorption Energies. Relative energies of CO_2 chemisorption by the formation of lactone groups on each of the graphene surfaces calculated at the UB3LYP/6-31G**, UCAM-B3LYP/6-31G**, and UMP2/6-31G** levels of theory, experimental observations and previous theoretical predictions are listed in Table 2. The relative energies are calculated using E(graphene-CO_2) {E(CO_2)+E(graphene)} for both chemisorption and physisorption. Here, the absolute energies are chosen from the ground electronic state. The geometries of base and graphene models at all possible high spin electronic states are fully optimized and their absolute energies at the UB3LYP/6-31G** level of theory are listed in Table 3. The ground states are a triplet state for all graphene-C_{32} models and the $C_{40}CO_2$, B model, and a quintet

Table 2. Absolute energies (E, in hartree), adsorption energies (ΔE, in kcal/mol) of CO_2 on graphene sheets at the UB3LYP, CAM-UB3LYP and UMP2/6-31G** levels of theory. Energies in parentheses include zero-point vibrational energy (ZPVE) corrections

			UB3LYP/6-31G**		CAM-UB3LYP/6-31G**		UMP2/6-31G**		Exp.	Previous study
			E	ΔE	E	ΔE	E	ΔE	B.E	B.E
Base	CO_2		-188.580940		-188.512845		-188.107309			
	C_{32}		-1218.609971		-1217.907576		-1215.040313			
	C_{40}		-1523.338060		-1522.466395		-1518.339457			
Chem	$C_{32}CO_2$	A	-1407.296267	66.1(62.3)	-1406.538213	73.9(70.2)				
	$C_{32}(CO_2)_6$		-2350.661701	59.2	-2349.621298	66.6				85[a]
	$C_{40}CO_2$	A	-1712.024002	65.9(62.3)	-1711.096891	73.8(70.8)			75[a]	95.7[b]
		B	-1712.068819	94.0(90.2)	-1711.139670	100.7(98.0)				32.3[c]
	$C_{40}(CO_2)_8$		-3032.825977	65.9	-3031.477133	71.2				39.7[d]
	$C_{40}(CO_2)_6$		-2655.399552	60.2	-2654.189302	67.5				
Phys	$C_{32}CO_2$	⊥	-1407.191721	0.3(0.2)	-1406.421699	0.8(0.7)	-1403.150982	2.1		⊥(‖)
		‖	-1407.191564	0.2(0.1)	-1406.422135	1.1(0.9)	-1403.152942	3.3	4.1[e]	3.5[g]
	$C_{40}CO_2$	⊥	-1711.919515	0.3(0.2)	-1710.980646	0.9(0.7)	-1706.449951	2.0	0.55[f]	1.4 (3.4)[h]
									4-9[a]	0.5[b]
		‖	-1711.919337	0.2(0.1)	-1710.981019	1.1(0.9)	-1706.451553	3.0		3.0 (3.1)[c]
										1.2[d]

[a]Ref 12: The most stable complex formed by the chemisorption of CO_2 on the graphene edge sites by the lactone group. [b]Ref 18. [c]Ref 20. [d]Ref 21: for the chemisorption of CO_2 on the monovacancy site. [e]Ref 26. [f]Ref 11: for the physisorption of CO_2 on SWNT. [g]Ref 10. [h]Ref 15

Table 3. Multiplicities (M), $<S^2>$ values, the differences $<S^2>$ - S(S+1), and absolute energies(in hartree) of bases and graphene models at different electronic states at the UB3LYP/6-31G** level of theory

M	$<S^2>$	$<S^2>$ - S(S+1)	Base(C₃₂)	Chem (C₃₂CO₂)	$<S^2>$	$<S^2>$ - S(S+1)	Base(C₄₀)	Chem (C₄₀CO₂, A)	Chem (C₄₀CO₂, B)
15	56.08	0.08	-1218.268855		56.13	0.13	-1523.071587		
13	42.09	0.09	-1218.346183	-1407.030388	42.10	0.10	-1523.146310	-1711.834697	
11	30.06	0.06	-1218.393518	-1407.078002	30.10	0.10	-1523.197949	-1711.887518	
9	20.09	0.09	-1218.438277	-1407.128142	20.10	0.10	-1523.255653	-1711.936449	-1711.932522
7	12.03	0.03	-1218.503577	-1407.185388	12.10	0.10	-1523.306934	-1711.992697	-1711.984935
5	6.10	0.10	-1218.549203	-1407.240753	6.04	0.04	-1523.338060	-1712.024002	-1712.037357
3	2.02	0.02	-1218.609971	-1407.296267	2.08	0.08	-1523.295810	-1711.982407	-1712.068819
1	0	0.00	-1218.548851	-1407.234440	0	0.00	-1523.251414	-1711.923195	-1712.008035

state for all other graphene-**C₄₀** models. The spin contamination in the UB3LYP wave function is not significant as pointed out by Sarofim and coworkers.[27] Results at the UCAM-B3LYP/6-31G** level of theory are listed in Table S1 of supplemental material. The energy of weakly bound systems such as physisorption energy predicted by B3LYP is generally lower than that calculated by MP2. Therefore, a long-range corrected (LC) DFT method (CAM-B3LYP) is used here for better description.

The chemisorption of CO_2 by lactone group formation on graphene-**C₃₂** is predicted at the UB3LYP/6-31g** level of theory to have an energy of 66.1 kcal/mol at site A. This is within the range of experimental observations (75-24 kcal/mol).[12] The UCAM-B3LYP binding energy is predicted to be 7.8 kcal/mol higher (73.9 kcal/mol) than UB3LYP result. CO_2 chemisorption energies on graphene-**C₄₀** are predicted to be 65.9 kcal/mol at site A and 94.0 kcal/mol at site B. The values are increased to be 73.8 kcal/mol (site A) and 100.7 kcal/mol (site B) at the UCAM-B3LYP level of theory. After ZPVE correction, the binding energis are reduced to 70.3 and 98.0 kcal/mol. To eliminate or minimize the site dependency, the chemisorption energies assuming high pressure have been estimated using graphene models fully covered by CO_2 on every possible adsorption site, that is, C₃₂(CO₂)₆, C₄₀(CO₂)₆ and C₄₀(CO₂)₈ as shown in Figure 3. The UB3LYP binding energy is calculated to be 65.9 kcal/mol for C₄₀(CO₂)₈, which is the same with the result of C₄₀CO₂ (site A), while the chemisorption energies for C₃₂(CO₂)₆ and C₄₀(CO₂)₆ are predicted to be little lower. The UCAM-

B3LYP binding energy is predicted to be 71.2 kcal/mol. The adsorption energy dependency for the lactone system with the C-O oriented towards the center of the edge line or outwards has been also tested in Table S2 and Figure S2. of supplemental material and the values are varied from 71.2 kcal/mol to 72.1 kcal/mol. This result is in reasonably good agreement with the experimentally observed 75 kcal/mol.

Physisorption energies of CO_2 on each of the graphene surfaces are calculated at various levels of theory, and are compared with experimental observations and previous theoretical predictions in Table 2. At the UB3LYP level of theory, the predicted physisorption energies (0.2-0.3 kcal/mol) are significantly underestimated relative to experimental results (4.1 kcal/mol)[26] and do not differ greatly with the size of the graphene model or the configuration, ⊥ or ||. The DFT method improved for weakly bound systems (UCAM-B3LYP) predicts physisorption energies of 0.8 and 1.1 kcal/mol for the ⊥ and || configurations, respectively, on C₃₂CO₂ model. While improved, the result remains an underestimate. The single-point UMP2 adsorption energies of all the graphene models (2.0-2.1 kcal/mol for the ⊥ configuration and 3.0-3.3 kcal/mol for the || configuration) are in reasonably good agreement with experimental observations. The larger binding energy in the parallel configuration can be explained by quadrupole-quadrupole interactions between the CO_2 and the C-C bonds on the graphene's surface. Overall, the size of the graphene model is shown not to be important to describing physisorption energy, while consideration of electron correlation effects (as by the UMP2 method) is very

    (a) C₃₂(CO₂)₆   (b) C₄₀(CO₂)₆   (c) C₄₀(CO₂)₈
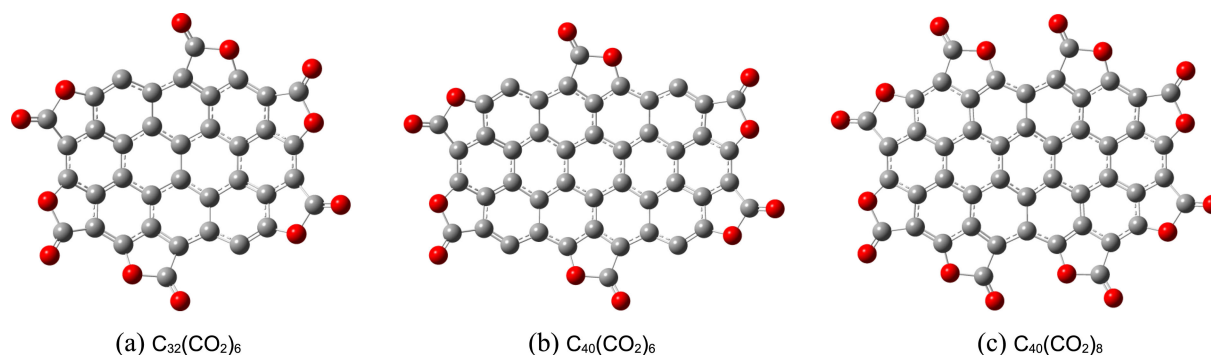
Figure 3. The geometries of graphene models fully covered by CO_2; (a) C₃₂(CO₂)₆ (b) C₄₀(CO₂)₆ (c) C₄₀(CO₂)₈.

important.

Conclusion

The geometric parameters and energies of the chemisorption and physisorption of CO_2 on graphene were calculated at various levels of theory. The formation of lactone groups is the most exothermic process in CO_2 adsorption on graphene and chemisorption by this route was investigated here. At the UCAM-B3LYP level of theory, the CO_2 chemisorption energies on graphene-C_{40} assuming high pressure are predicted to be 71.2-72.1 kcal/mol for the lactone systems depending on various C-O orientations. This result is in reasonably good agreement with the experimentally observed 75 kcal/mol.

Two configurations of physisorption, parallel ($\parallel$) and perpendicular ($\perp$), that result depending on the direction of CO_2's approach to the graphene surface were also optimized. Single-point UMP2 adsorption energies were calculated to be 2.0-2.1 kcal/mol for the $\perp$ configuration, and 3.0-3.3 kcal/mol for the $\parallel$ configuration in each of the considered graphene models. These results are in reasonably good agreement with experimental observations and previous theoretical predictions. The size of the graphene models was shown not to have too great an effect on the physisorption energy, while consideration of electron correlation effects was shown to be very important.

References

1. Service, R. F. *Science* **2004**, *305*, 962.
2. Rao, A. B.; Rubin, A. R. *Environ. Sci. Technol.* **2002**, *36*, 4467.
3. Jiang, J.; Sandler, S. I. *J. Am. Chem. Soc.* **2005**, *127*, 11989.
4. Dillon, A. C.; Jones, K. M; Bekkedahl, T. A.; Kiang, C. H.; Bethune, D. S.; Heben, M. J. *Nature* **1997**, *386*, 377.
5. Liu, C.; Fan, Y. Y.; Liu, M.; Cong, H. T.; Cheng, H. M.; Dresselhaus, M. S. *Science* **1999**, *286*, 1127.
6. Chen, P.; Wu, X.; Lin, J.; Tan, K. L. *Science* **1999**, *285*, 91.
7. Ye, Y.; Ahn, C. C.; Witham, C.; Fultz, B.; Liu, J.; Rinzler, A. G.; Colbert, D.; Smith, K. A.; Smalley, R. E. *Appl. Phys. Lett.* **1999**, *74*, 2307.
8. Kong, J.; Franklin, N. R.; Zhou, C.; Chapline, M. G.; Peng, S.; Cho, K.; Dai, H. *Science* **2000**, *287*, 622.
9. Collins, P. G.; Bradley, K.; Ishigami, M.; Zettl, A. *Science* **2000**, *287*, 1801.
10. Zhao, J. J.; Buldum, A.; Han, J.; Lu, J. P. *Nanotechnology* **2002**, *13*, 195.
11. Cinke, M.; Li, J.; Bauschlicher, C. W., Jr.; Ricca, A.; Meyyappan, M. *Chem. Phys. Lett.* **2003**, *376*, 761.
12. Montoya, A.; Mondragon, F.; Truong, T. N. *Carbon* **2003**, *41*, 29.
13. Matranga, C.; Chen, L.; Smith, M.; Bittner, E.; Johnson, J. K.; Bockrath, B. *J. Phys. Chem. B* **2003**, *107*, 12930.
14. Novoselov, K. S.; Geim, A. K.; Morozov, S. V.; Jiang, D.; Zhang, Y.; Dubonos, S. V.; Grigorieva, I. V.; Firsov, A. A. *Science* **2004**, *306*, 666.
15. Yim, W. L.; Byl, O.; Yates, J. T., Jr.; Johnson, J. K. *J. Chem. Phys.* **2004**, *120*, 5377.
16. Radovic, L. R. *Carbon* **2005**, *43*, 907.
17. Allouche, A.; Ferro, Y. *Carbon* **2006**, *44*, 3320.
18. Xu, S. C.; Irle, S.; Musaev, D. G.; Lin, M. C. *J. Phys. Chem. B* **2006**, *110*, 21135.
19. Huang B.; Li, Z.; Liu, Z.; Zhou, G.; Hao, S.; Wu, J.; Gu, B-L.; Duan, W. *J. Phys. Chem. C.* **2008**, *112*, 13442.
20. Cabrera-Sanfelix, P. *J. Phys. Chem. A* **2009**, *113*, 493.
21. Liu, Y.; Wilcox, J. *Environ. Sci. Technol.* **2011**, *45*, 809.
22. Mishra, A. K.; Ramaprabhu, S. *AIP Advances* **2011**, *1*, 032152.
23. (a) Becke, A. D. *J. Chem. Phys.* **1993**, *98*, 5648. (b) Lee, C.; Yang, W.; Parr, R. G. *Phys. Rev.* **1988**, *B37*, 785.
24. Yanai, T.; Tew, D. P.; Handy, N. C. *Chem. Phys. Lett.* **2004**, *393*, 51.
25. Frisch, M. J.; Trucks, G. W.; Schlegel, H. B.; Scuseria, G. E.; Robb, M. A.; Cheeseman, J. R.; Scalmani, G.; Barone, V.; Mennucci, B.; Petersson, G. A.; Nakatsuji, H.; Caricato, M.; Li, X.; Hratchian, H. P.; Izmaylov, A. F.; Bloino, J.; Zheng, G.; Sonnenberg, J. L.; Hada, M.; Ehara, M.; Toyota, K.; Fukuda, R.; Hasegawa, J.; Ishida, M.; Nakajima, T.; Honda, Y.; Kitao, O.; Nakai, H.; Vreven, T.; Montgomery, J. A.; Peralta, J. E., Jr.; Ogliaro, F.; Bearpark, M.; Heyd, J. J.; Brothers, E.; Kudin, K. N.; Staroverov, V. N.; Kobayashi, R.; Normand, J.; Raghavachari, K.; Rendell, A.; Burant, J. C.; Iyengar, S. S.; Tomasi, J.; Cossi, M.; Rega, N.; Millam, J. M.; Klene, M.; Knox, J. E.; Cross, J. B.; Bakken, V.; Adamo, C.; Jaramillo, J.; Gomperts, R.; Stratmann, R. E.; Yazyev, O.; Austin, A. J.; Cammi, R.; Pomelli, C.; Ochterski, J. W.; Martin, R. L.; Morokuma, K.; Zakrzewski, V. G.; Voth, G. A.; Salvador, P.; Dannenberg, J. J.; Dapprich, S.; Daniels, A. D.; Farkas, Ö.; Foresman, J. B.; Ortiz, J. V.; Cioslowski, J.; Fox, D. J. *Gaussian 09, Revision A*; Gaussian, Inc., Wallingford CT, 2009.
26. Vadali, G.; Ihm, G.; Kim, H. Y.; Cole, M. W. *Surf. Sci. Rep.* **1991**, *12*, 133.
27. Montoya, A.; Truong, T. N.; Sarofim, A. F. *J. Phys. Chem. A* **2000**, *104*, 6108.